Granular flows in the centrifuge

M.A. Cabrera & W. Wu
Institute for geotechnical engineering, University of Natural Resources and Life Sciences (BOKU), Vienna, Austria

J. Mathews
Formerly at Institute for geotechnical engineering, University of Natural Resources and Life Sciences (BOKU), Vienna, Austria

ABSTRACT: By varying the acceleration field, the granular flows enable the simulation of flow configurations with a low cost and testing time, and high repeatability. However the scaling principles employed in such flows remain poorly studied and require several considerations with respect to the acceleration field. This paper presents a review of the mass flow rate of granular flows under a centrifugal acceleration field, in two experimental models. First, a silo model is developed to study the discharge rate of dry granular flows. Mass flow rates are continuously measured during discharge, showing a clear relationship between the scaling principle and the induced driving force. Second, a channel model is developed to study free-surface mass flows flowing down an inclined plane. The model show a clear relationship between the driving acceleration field and the flow characteristics, and contributes to the study of scaling principles of large-scale granular phenomena at a reduced scale.

1 INTRODUCTION

Centrifuge induces a centrifugal acceleration field by rotating a scale model at a constant angular velocity ω, resulting in a centrifugal acceleration a_{cf} in the radial direction. At the point where the centrifugal acceleration exceeds Earth's gravity g by a factor of N, the self-load of a body and the gravity-driven processes are deflected towards the radial direction and are augmented by a proportional factor. In geotechnical engineering, centrifuge modelling is used in the study of the stress-strain behaviour of granular materials by varying a_{cf} (Taylor, 1995), and applied in the study of slope stability, soil-structure interaction, foundation systems, soil reinforcement, tunnelling, unsaturated soil mechanics, and more recently in the study of granular flows. The good agreement between centrifuge models and field observations led to the adoption and development of centrifuge modelling as a reliable experimental technique for the study of complex stress-strain materials and their role in coupled systems (Craig, 2001).

Granular flows are common in natural hazards (e.g. debris flows, mud flows, rock avalanches, and snow avalanches) and industrial processes (e.g. food processing, and cement production) that involve the concentrated or loose motion of discrete particles when dry or mixed with a fluid.

In these flows, the stress-strain behaviour of the granular media is strongly linked with the momentum transfer during flow. A common characteristic of the granular flows mentioned above is that gravity is the main driving force, defining the packing density during flow and the intensity and duration of the main interactions between particles and their sur-

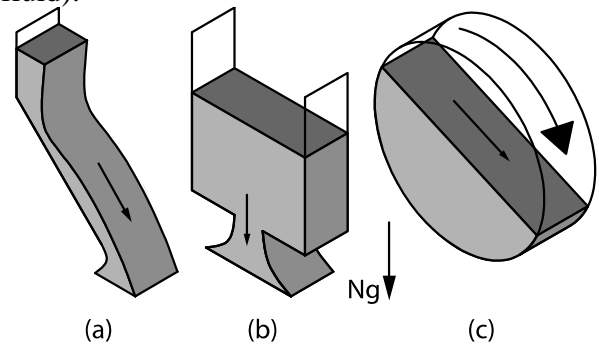rounding media (particle-particle, particle-fluid, fluid-fluid).

Figure 1. Flow configurations studied in the centrifuge. (a) Granular flow down an inclined plane, (b) granular flow out of a silo, and (c) granular flow in a rotating drum.

At the same time, gravity delimits the occurrence of phase separation, inverse segregation, and mass consolidation. Therefore, centrifuge modelling offers the opportunity to study the role and scaling of gravity in the understanding of the physics of granular flows. The research of granular flows in a geotechnical centrifuge is still in its early days. The first models are reported in 2006 on the study of granular flows down an inclined plane (Vallejo et al., 2006), and on the creeping granular motion in a rotating drum (Arndt et al., 2006). Recent research broadens the model flow configurations, testing granular flows down curved channels (Bowman et al., 2010, and Imre et al., 2010), and studying the kinematics involved during the emptying of a silo (Dorbolo et al., 2013, and Mathews, 2013). In this paper we focus on the discharge characteristics during the emptying of a silo and the flow of granular material down an inclined plane (Fig. 1).

1.1 Scaling principles.

The mass, momentum, and energy balance of a granular flow are formulated in terms of the flow pressure p, flow thickness h, and flow velocity u (Andreotti et al, 2013). Under the effects of a centrifugal acceleration field the flow pressure is related to the static self-weight of a column of grains, being augmented by the acceleration field in the radial direction (compound action of the centrifugal, Coriolis, and inertial acceleration terms). Assuming that the centrifugal acceleration field does not vary with the radius and can therefore be described as a_{cf}, the integration of the self-weight of a unit cross-section column in the *model* becomes $\sigma_z = \rho N g h$ (Garnier et al, 2007), where ρ is the density of the soil column and h its height. Assuming that the material employed in the scale model shares the same density ρ as a field *prototype*, the scaling principle of stresses yields $\sigma_{z,m} \equiv \sigma_{z,p}$ where the subscripts m and p relate to the stresses in the model and in the prototype, respectively. This assumption results in a height equivalence of $h_m \equiv h_p/N$, for a column of granular material, which is commonly related with the scaling of the flow thickness (Milne et al, 2012, Kailey, 2013, and Bryant et al., 2015). Furthermore, a similar scaling principle as for the vertical stress is formulated for the flow velocity in the form of $u_m \equiv u_p$ (Vallejo et al., 2006). In a free-surface flow, the Froude number Fr relates the speed of propagation of the flow with the gravitational wave speed (Gray & Edwards, 2014), in the form:

$$\text{Fr} = u / \sqrt{gh\cos\zeta} \qquad (1)$$

where ζ is the angle of the inclined plane. The velocity scaling principle can be reviewed by defining an equivalence between the $\text{Fr}_m \equiv \text{Fr}_p$. In this formulation the scaling principle of velocity results only if the flow thickness equivalence mentioned above is assumed. However, Brucks et al. showed that for experiments on granular flows in a rotating drum the flowing thickness remains constant in a centrifugal acceleration field (Brucks et al., 2007).

1.2 Silo discharge

In order to predict the mass flow rate from a silo ψ, Beverloo developed a correlation using dimensional analysis, and calculated ψ as function of the bulk material density ρ_b, gravity g, outlet diameter D and material friction μ (Beverloo et al., 1961).

Plotting this relationship for a range of orifice diameters in the form $W^{2.5}$ against D shows that the relationship is linear with a non-zero intercept of $W^{2.5}$ on the D axis. Tests with mono-sized particles of different diameters show that the size of the intercept is proportional to particle diameter d and leads to the following correlation:

$$\psi = C\rho_b \sqrt{g}(D-kd)^{2.5} \qquad (2)$$

where C is a coefficient which is found to be almost constant despite being expected to be proportional to friction, and k is a coefficient which usually ranges from $1.0 - 1.5$ for spherical particles and is greater for non-spherical particles.

The Beverloo correlation may be modified for rectangular outlets by maintaining dimensional consistency and considering that ψ increases linearly with the silo thickness l, yielding:

$$\psi = C\rho_b \sqrt{g}(l-kd)(W_0-kd)^{1.5} \qquad (3)$$

where W_0 is the width of the outlet. Equation 3 has been used to predict the flow rate from the model silo in the centrifuge model.

The Beverloo correlation may be modified for silos with hoppers by considering the work of Rose & Tanaka (1956), where the influence of the angle of the stagnant zone was investigated. The following correlation was reported:

$$\psi \propto (\tan\beta \tan\psi_d)^{-0.35} \qquad (4)$$

when $\beta < 90 - \psi_d$ and where β is the hopper half angle and ψ_d is the angle between the stagnant zone boundary and the horizontal.

This has been used to modify the Beverloo correlation for a silo which is not flat bottomed and can be incorporated into the Beverloo equation in the following way:

$$\psi = \psi_B F(\beta,\psi_d) \qquad (5)$$

where ψ_B is the discharge rate using the Beverloo correlation and $F(\beta, \psi_d)$ is:

$$F = (\tan\beta \tan\psi_d)^{-0.35} \quad \text{for } \beta < 90 - \psi_d \qquad (6)$$

$$F = 1 \qquad\qquad\qquad \text{for } \beta > 90 - \psi_d \qquad (7)$$

Beverloo's equation has proven robust and is widely used, however few experiments can be found which test its inherent prediction that the discharge rate ψ of cohesionless media is proportional to the square root of the acceleration due to gravity. Investigations of the influence of gravity on bulk solids include numerical investigations by Chung & Ooi (1956) and physical investigations by Dorbolo et al. (2013).

2 METHODS

Experiments are performed in the beam centrifuge (Trio-Tech 1231) in the institute of geotechnical engineering (IGT) at the University of Natural Resources and Life Sciences (BOKU), Vienna, Austria. The centrifuge has a nominal radius of 1.31 m, maximum design acceleration of $200g$, maximum load capacity of 10,000kg·g, and is able to hold maximum model dimensions of 0.54 m × 0.56 m × 0.56 m (W×L×H).

The centrifuge is controlled via 56 slip-rings placed around the rotation axis. Angular velocity, energy supply, and signal control are maintained from the centrifuge's control room. In-flight sensor data is recorded using two computers and a data acquisition system is placed near the rotation axis of the centrifuge. The computers enable higher sampling frequencies and greater model instrumentation.

2.1 Materials

The material used in the centrifuge experiments is a bi-disperse mixture of silver and black glass beads (Fig. 2). The glass beads are produced by Sigmund Lindner GmbH, Warmensteinach, Germany, and have well defined material properties and limits of variability. The main properties are detailed in Table 1. For the free-surface flows down an inclined plane, experiments are performed with only the silver glass beads of 1.45 mm diameter.

Figure 2. Photograph of the bi-disperse mixture of glass beads.

Table 1. Properties of bi-disperse mixture of silver and black glass beads presented in Figure 2.

Property	
Material density ρ [g/cm3]	2.750
Bulk density ρ_b [g/cm3]	1.52
Particle diameter, black d_1 [mm]	3.15 ± 0.1
Particle diameter, silver d_2 [mm]	1.45 ± 0.1
Void ratio e [-]	0.809
Coefficient of uniformity U [-]	2.17
Friction angle φ_0 [°]	22

2.2 Experimental apparatus

2.2.1 Silo model

The model silo (Fig. 3) has an outlet width $W_0 = 30$ mm, thickness $l = 100$ mm, and width $W = 150$ mm. Two configurations of silo are tested; flat bottomed (shown) and 30° hopper (measured from the vertical). The distance between the silo outlet and the top of the stored material, when full, is approximately 300 mm. The silo has aluminum lateral walls 100 mm deep, an aluminum back wall, and a 30 mm thick Plexiglass GS front window. The silo is designed so that all internal faces are smooth.

Model instrumentation. In these tests the only instrumentation used is a pair of load cells located below the collection bucket. The load cells record the force exerted by the collection bucket and its contents at a rate of 50 Hz.

Test routine. Material is poured into the model silo at $1g$ through a funnel designed for use with the model silo. The mass of material in the silo is calculated by measuring the mass of the storage bucket and funnel before and after filling. The silo is then accelerated and held at an angular velocity corresponding to $5g$, $10g$ or $15g$ at the silo outlet (with a radial distance $R_i = 1.075$ m). Tests at 1g are made whilst the centrifuge is stationary.

Silo discharge is initiated by activating a servo-motor once the centrifuge has reached the required angular velocity. Activating the motor causes a spindle attached to the motor to pull a pin which releases a spring-loaded sliding silo door which moves away from the silo outlet leaving it unobstructed. When the silo centrifuge model is opened, the material discharges from the silo into a bucket. Load cells measure the load exerted by the bucket and its contents. Once discharge is complete, the centrifuge is decelerated until the beam is stationary. The load cell data then stops being recorded and the centrifuge is turned off.
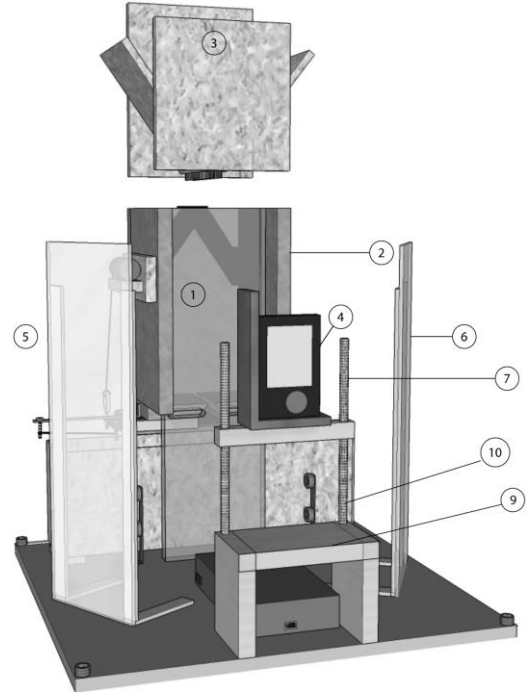

Figure 3. Sketch of model silo outside of centrifuge, 1-acrylic window, 2-side wall, 3-filling funnel, 4-camera, 5, 6-LED array, 7-camera stand, 9-vertical roller, 10-collection bucket.

Tests at a specific acceleration are repeated until 3 tests with less than 5% variation in discharge rate are obtained. For the calculation of the Beverloo mass flow rate in Eq. 3 the bi-disperse glass beads are considered to have mean particle diameter $d^* = 2.3$ mm, with discharge coefficients $C = 1.03$ and $k = 1$.

2.2.2 Channel model

In addition to this brief review of the main characteristics of the model, a detailed description of the scale model and its instrumentation is presented in Cabrera (2016). The experimental apparatus is designed in two main sections. At the first section, a silo is connected to a pivoting system lying over the centrifuge arm. This connects to the scale model through a flexible pipe. The scale model is located in one of the centrifuge's two swinging baskets; the incoming material flows down an inclined plane within the model and is collected in a wooden box at the end of the incline (see Fig. 4).

The silo is a 75 mm×250 mm cylindrical PVC tube (D×L) with an opening of 32mm×50 mm, at

one of the circular tops, closed by the triggering gate. The mechanism is triggered by a servo-motor that pulls a pin, which releases a wedge that holds a plate closing the silo. Once the wedge is released, the plate is pulled by a loaded spring leaving the material to flow freely through the feeding tube and reach the inclined plate in the model.

The inclined plate is an 80 mm×400 mm×3 mm aluminium plate (W×L×T), confined between a 15 mm thick aluminium wall and a 30 mm thick Plexiglass GS window (creating a rectangular channel cross-section). A 2 mm thick rubber sheet covers the inclined aluminium plate. The plate is supported by two bars (8 mm in diameter) crossing and laying through the lateral walls, allowing the adjustment of the inclination angle ζ by fixing the elevation of the bars. The inclination can vary from 10° to 50°, in steps of 5°.

At the end of the inclined plate the material is collected in a wooden box of 76 mm×80 mm×480 mm (W×L×H). The collection box is confined between the lateral walls by four single-ball bearings (25.4 mm in diameter), allowing displacements to occur only in the direction of the flow (lateral displacements are constrained). The transition from the inclined plate to the collection box is done by two thin cellulose acetate foils.
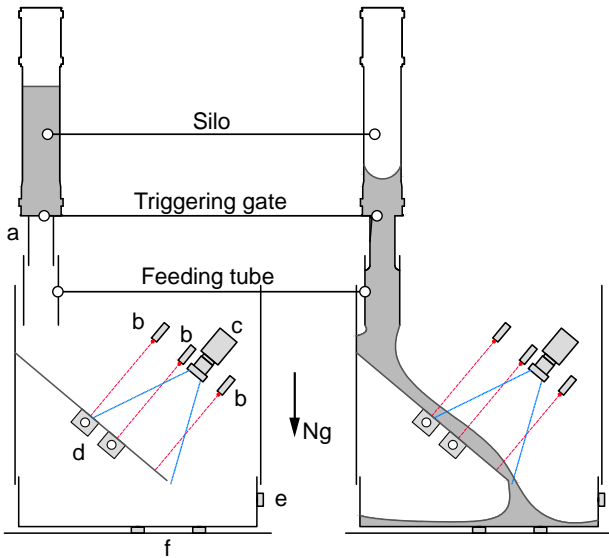

Figure 4. Sketch of the channel model for free surface flows. Instrumentation: a. photo transistor, b. point-height lasers, c. high-speed camera, d. basal load cells, e. horizontal load at the collection box, and f. vertical load cells at the collection box.

Model instrumentation. The scale model is instrumented from the moment the triggering gate opens until the material deposits in the collection box. For the purpose of the current paper a bottom sensor-group of load cells (with a nominal force of 1 kN) is set in contact with the collection box measuring the horizontal and vertical loads during the discharge of the flowing mass. In this arrangement, two load cells are located under the box at the thirds of its length, and one is horizontally orientated in contact with the mid-height of the box (Fig. 4). During

experiments, load cells are recorded at a sampling rate of 19.4 kHz by a QuantumX MX1615B data acquisition system.

Test routine. The glass beads flows are tested at angles between $20° \leq \zeta \leq 50°$. At each angle, experiments are performed at $1g$, $10g$, and $20g$. The $1g$ experiments (outside the centrifuge) bring a reference behaviour to compare with the centrifuge experiments. All experiments are performed with 1000.3g of glass beads loaded in the silo. The inclined plate is orientated in the $r^+\theta^+$ direction in the centrifuge basket, resulting in dense flows driven by the summation of the centrifugal acceleration and the Coriolis acceleration with components pointing inwards towards the inclined plate.

3 RESULTS

3.1 *Mass flow rate in the silo*

When the silo is opened, material begins to flow from the silo though the silo outlet into the collection bucket. The two load cells placed beneath the collection bucket record the increase in load which results from the material entering the collection bucket. The results show that the increase in load during discharge is linear and impact forces do not distort the linear increase in load (Fig. 5).

The results show that material flows from the silo with a hopper at a greater rate than material from the flat bottomed silo. By considering the material density and the centrifugal acceleration, the mass flow rate of the glass beads from the silo-centrifuge model can be calculated from the rate of increase of the signal from the load cells. The observed mass flow rates are compared to either the Beverloo model for flat-bottomed silos (Eq. 3), or to the adjusted Beverloo model for the silo with 30° hopper (Eq. 5).

3.2 *Mass flow rate in an inclined plane*

During the discharge at the end of the inclined plane, the material deposits into one side of the box, making it tilt towards the loaded side. This uneven deposition is registered from the load cells from the moment of the first impact, unloading the load cell that lays farther from the deposition point, making the one near the deposition point to hold the full load of the flowing material. At the load cell near the deposition point, the discharge of the material is characterized by a smooth beginning, followed by a stable loading rate, and finishing with a smooth transition towards the final force exerted by the deposited material. Because of the uneven distribution, the analysis of the discharge forces is simplified to the measurements of the load cell near the deposition point. Furthermore, the horizontal load cell in contact with the collection box did not register the discharge of the material. This indicates the vertical loading process.

The rate of the loading process q, at the collection box, is measured as the gradient of the loading measurements. A linear approximation is assumed to be representative of the discharge at the end of the incline, and is divided by the centrifugal acceleration in the flowing material, yielding the *mass flow rate* at the end of the inclined plate $\psi = q/a_{cf}$ (Fig. 6)

4 DISCUSSION

4.1 *Mass flow rate of a silo*

Figure 7 presents an equivalent mass flow rate ψ_{eq} defined as the mass flow rate divided by the non-gravitational terms of the Beverloo correlation (Eq. 8). This is plotted against $g^{0.5}$. From Equation 8 it is clear that if the mass flow rate is described by the Beverloo correlation, then the equivalent discharge rate plotted against the square root of the gravity will have gradient 1 and intercept 0.

$$\psi_{eq} = \frac{\psi_{observed}}{\psi_{Bev}/\sqrt{g}} = \frac{\psi_{observed}}{C\rho_b(l-kd)(W_0-kd)^{1.5}} \quad (8)$$
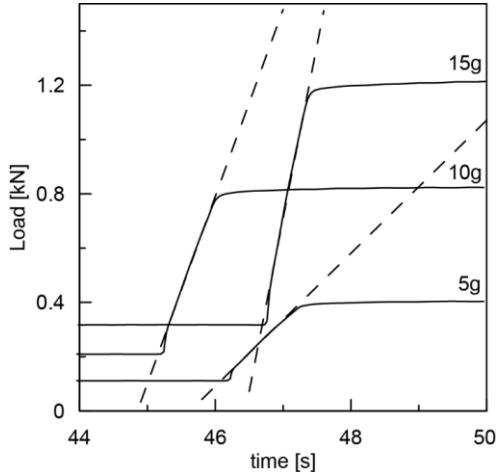
Figure 5. Typical load cell result, Glass beads, Flat bottomed silo. Dashed line shows gradient during silo discharge.
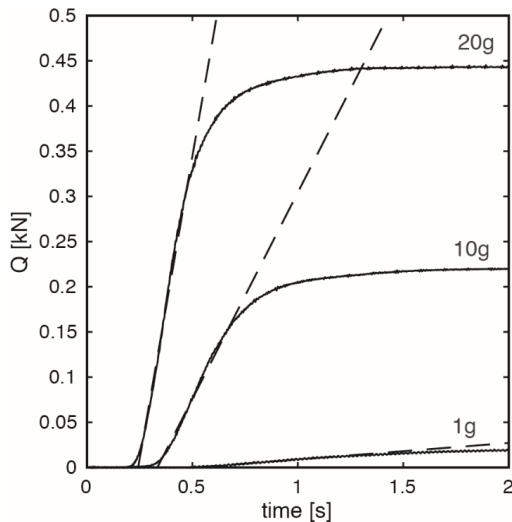
Figure 6. Discharge load Q measured at the collection box for glass beads flows at $\zeta = 30°$. The dashed line represents the loading rate q at variable acceleration levels in the model.

The high coefficients of determination suggest that the discharge rate is linearly proportional to the square root of the gravity. The average gradient of the discharge rate is 0.88 for the flat bottomed silo, implying that $\psi \propto 0.77(g^*)^{0.5}$, and 0.97 for the silo with 30° hopper, implying that $\psi \propto 0.94(g^*)^{0.5}$. This range of gradients shows that discharge rates are more sensitive to gravity in silos with hoppers than in flat bottomed silos. Possible mechanisms to explain this include the role of locking or jamming mechanisms between the grains of the stored material, which are governed by gravitational forces.
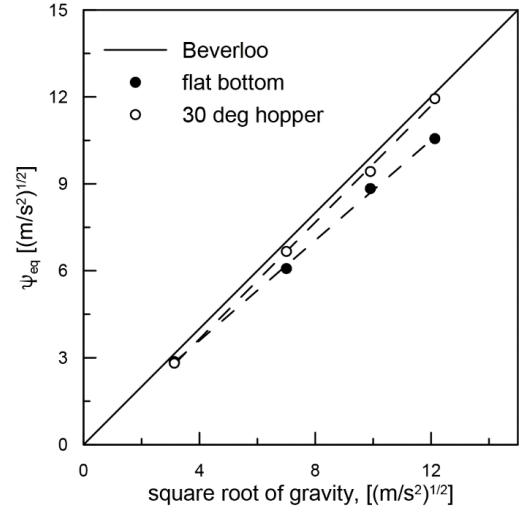
Figure 7. Equivalent mass flow rate ψeq of the silo with flat bottom and a 30° hopper.

4.2 *Mass flow rate on an inclined plane*

Figure 8 presents the mass flow rate as a function of the angle ζ at the inclined plate and at variable acceleration levels Ng. For the centrifuge experiments ψ increases between the range of $20° \leq \zeta < 30°$, and then for $\zeta \geq 30°$ ψ remains constant. Furthermore, ψ scales with effective acceleration and has a greater discharge rate for experiments at $20g$.

Given that for all experiments the silo opening remains constant, the inflow of material is controlled by the governing acceleration at the silo opening (with a radial distance of $R_i = 0.74$ m). The mass flow rate at the triggering gate ψ_{silo} is calculated with Beverloo's equation for silos (see Eq. 3). The coefficients in Eq. 3 agree with those reported for silo experiments ($C = 1.03$ and $k = 1.0$).

For the centrifuge experiments, the case where $\psi < \psi_{silo}$ corresponds to the compound acceleration of a_{cf} and $a_{coriolis}$ over the flowing material. This compound acceleration enhances the frictional dissipation through the feeding tube and along the inclined plate. Nevertheless, for inclinations of $\zeta \geq 30°$ a constant mass flow rate is registered at the collection box, being a function of ψ_{silo}. This last point reinforces the conclusion that inertial processes in the centrifuge scale by a factor of $N^{0.5}$ as presented by Bryant et al. (2015) and implied by Bowman et al. (2013) in the determination of the semi-empirical velocity profile for coarse grained debris flows (Takahashi, 2007).
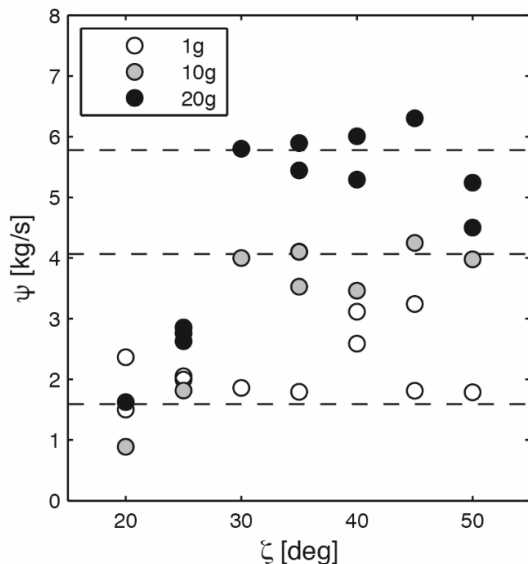
Figure 8. Mass flow rate at the collection box as a function of ζ and Ng. The horizontal dashed-lines show the supply mass flow rate ψ_{silo} at the opening of the silo calculated by Eq. 3.

4.3 *Scaling of the mass flow rate in a centrifuge*

From the experimental results presented in Figs. 7 and 8, it is reasonable to conclude that the mass flow rate ψ of granular flows under the effects of a centrifugal acceleration field is equivalent to a factor of $N^{0.5}$. For the experiments presented here, the Beverloo equation (see Eq. 3) accounts for the effect of the driving acceleration by a similar factor. Because of this similarity, we conclude that if experiments are performed on granular assemblies discharging with a controlled outflow, the resultant discharge is scaled by $a_{cf}^{0.5}$.

As a result of these experimental tests, it becomes clear that by increasing a_{cf} in a model with a granular flow, the resultant velocity increases by a factor of $N^{0.5}$. This work therefore lends support to the scaling principle for the inertial velocity, in order to account for the inertial contribution of the centrifugal acceleration field.

5 CONCLUSIONS

This paper presents a review of granular flows in a silo and granular flows down an inclined plate, each under the effects of a centrifugal acceleration field. The granular flows are composed of a bi-disperse set of glass beads in the silo model, and a mono-disperse set of glass beads in the channel model. The mass flow rate ψ in both experimental models is calculated directly from measuring load beneath the collection bucket, and show that by increasing the centrifugal acceleration a_{cf}, ψ scales by a factor of $N^{0.5}$. The experimental observations are related to the outflow discharge initiated by opening the silo (see Eq. 3), preserving the same scaling factor.

The validity of the $N^{0.5}$ scaling principle is of great importance for the study of granular flows in centri-

fuges. In particular, it will contribute to increasing insight and understanding of physical processes in a growing research field.

REFERENCES

Andreotti, B., Forterre, Y. and Pouliquen, O. 2013. Granular media. Between fluid and solid. Cambridge Univ Press.

Arndt, T Brucks, A Ottino, J and Lueptow, R. 2006. Creeping granular motion under variable gravity. Phys.Rev.E 74 031307

Beverloo, W. A., Leniger, H. A., and van de Velde, J. 1961. The flow of granular solids through orifices. Chem.Eng.Sc.260-269

Beverloo, W., Leninger, H., and van de Velde, J. 1961. The flow of granular solids through orifices. Chem. Eng.Sc. 260–269.

Bowman, E., Laue, J. and Springman, S. 2010. Experimental modelling of debris flow behaviour using a geotechnical centrifuge. Canadian Geotechnical Journal 47, 7, 742–762.

Brucks, A., Arndt, T., Ottino, J and Lueptow, R. 2007. Behavior of flowing granular materials under variable g. Phys.Rev. E 75.

Bryant, S., Take, W., Bowman, E., and Millen, M. 2015. Physical and numerical modelling of dry granular flows under coriolis conditions. Gotechnique 65, 3, 188–200.

Cabrera, M. 2016. Granular flows in rotating frames. PhD thesis, University of Natural Resources and Life Sciences, Vienna.

Chung, Y.-C., and Ooi, J. 2008. A study of influence of gravity on bulk behaviour of particulate solid. Particuology 6, 467 – 474.

Craig, W. 2001. The seven ages of centrifuge modelling. In Constitutive and Centrifuge Modelling: Two Extremes, S. Springman, Ed., A.A. Balkema publishers.

Dorbolo,S., Maquet, L., Brandenbourger, M., Ludewig, F., Lumay, G., Caps, H., Vandewalle, N., Rondia, S., van Loon, J., Dowson, A., and Vincent-Bonnieu, S. 2013. Influence of the gravity on the discharge of a silo. Gran.Mat.15, 263 – 273.

Garnier, J., Gaudin, C., Springman, S., Culligan, P., Goodings, D., Konig, D., Kutter, B., Phillips, R., and Thorel, L. 2007. Catalogue of scaling laws and similitude questions in geotechnical centrifuge modelling. Int. J.Phys.Mod.Geot.7, 3, 1–23.

Gray, J. and Edwards, A. 2014. A depth-averaged µ(i)rheology for shallow granular free-surface flows. J.Fl.Mech.755 503–534

Imre, B., Laue, J. and Springen, S. 2010. Fractal fragmentation of rocks within sturzstroms: insight derived from phys. exp. within the geotech. drum centrifuge. Gran. Mat.12, 267–285.

Kailey, P. 2013. Debris flows in New Zealand alpine catchments. PhD thesis, University of Canterbury.

Mathews, J. 2013 Investigation of Granular Flow using Silo Centrifuge Models. PhD thesis, Univ. fuer Bodenkultur, Vienna.

Milne, F., Brown, M, Knappett, J, and Davies, M 2012. Centrifuge modelling of hillslope debris flow initiation. Catena92 162-171

Rose, H. F., and Tanaka, T. October 23 1956 The Engineer (London) 208.

Takahashi, T. 2007 Debris flow: mechanics, prediction and countermeasures. Taylor & Francis, Leiden.

Taylor, R. 1995 Geotechnical Centrifuge Technology. Blackie.

Vallejo, L., Estrada, N., Taboada, A., Caicedo, B., and Silva, J. 2006. Numerical and physical modeling of granular flow. In Phys.Mod.Geot. Ng and Zhang, Eds., Taylor & Francis.